Nascent rotational distribution and the relaxation of the N2+ ion produced by double resonant multiphoton ionization

Nascent rotational distribution and the relaxation of the N_2^+ ion produced by double resonant multiphoton ionization

Asuka Fujii, Takayuki Ebata, and Mitsuo Ito
Department of Chemistry, Faculty of Science, Tohoku University, Sendai 980, Japan

Laser induced fluorescence (LIF) detection has been applied to measure the rotational distribution of the N_2^+ ion produced by double resonant multiphoton ionization of the N_2 molecule. By analysis of the LIF spectra of the generated N_2^+ ion, the rotational propensity rules of the photoionization of N_2 have been determined, which agree with theoretical prediction. The observed rotational intensity distribution shows relatively good agreement with the calculated result. Rotational relaxation of the N_2^+ ions by N_2 collision has also been measured. The rotational relaxation rate constant is almost equal to that of the vibrational relaxation and the selection rule "symmetric" (+)↔"symmetric"(+) has been found to be obeyed.

I. INTRODUCTION

Molecular photoionization is widely used to produce ions in a selected internal state and the state selectivity is much higher than that of the electron impact or discharge method. The state selectivity has been further improved by resonant enhanced multiphoton ionization (REMPI), where the internal state distribution of the ions is determined by the ionization from the intermediate state.[1-3] The vibrational state distribution of an ion produced by the photoionization has been extensively studied by photoelectron spectroscopy. However, ordinary photoelectron measurements do not have enough resolution to study the rotational state distribution. Only H_2[4-8] and NO[9-11] are the diatomic molecules whose photoelectron spectra were rotationally resolved. All the previous studies of the internal state distribution were based on the measurement of ejected photoelectrons. However, the direct observation of the nascent distribution of the ion itself, such as the measurement of the laser induced fluorescence spectrum (LIF), has never been performed. Since the resolution of the spectrum is determined by probing laser resolution, we can achieve much higher resolution than that of the conventional photoelectron measurement.[12] In addition, we can discuss in detail the rotational branching ratio by the rotational distribution of the LIF spectrum. This is a good advantage over the photoelectron study, where the intensity of the photoelectron is greatly affected by the relative angle of the direction of the laser polarization to that of the detection due to the anisotropy of the ejected electron.

In a previous work we measured the LIF spectra of the N_2^+ ions produced by (2 + 2)REMPI via the $a\,^1\Pi_g\,(v = 1)$ state of N_2 and tried to find the nascent rotational distribution of the N_2^+ ion.[13] However, in the (2 + 2) ionization, the N_2^+ ions produced are vibrationally distributed from $v = 0$ to $v = 7$. Furthermore, since the N_2 molecule in the $a\,^1\Pi_g$ state is ionized by the two photons, the rotational propensity rule is thought to be very complicated and the final ions produced are not only vibrationally, but also rotationally, distributed over the various levels.

In the present work we have applied the two-color double resonance method (two-color REMPI) to generate N_2^+ ions and measured the rotational distribution of N_2^+ by the laser induced fluorescence. The double resonance method has a great advantage over the "single" resonance method to produce a large amount of ions in a single vibronic level when we select the Rydberg state as a final resonant state. The generated ions are selectively distributed in the single vibronic state because of the similarity of the potentials between the Rydberg state and the ionic state.

Figure 1 shows the excitation and detection scheme. The potential curves are drawn using the parameters given by Huber and Herzberg.[14] We selected the $a\,^1\Pi_g\,(v = 1)$ state of N_2 as the first resonant state and the $c'\,^1\Sigma_u^+$ ($4p\sigma$ Rydberg) or $c\,^1\Pi_u$ ($3p\pi$ Rydberg) state as the second resonant state. N_2^+ ions were produced by one-photon absorption from the $c'\,^1\Sigma_u^+$ or $c\,^1\Pi_u$ state and their nascent rotational distribution was observed by the measurement of the LIF spectra of N_2^+ due to the $B\,^2\Sigma_u^+ \leftarrow X\,^2\Sigma_g^+$ transition. The observed rotational propensity rules agree well with the theoretical prediction. For the ionization from the $c'\,^1\Sigma_u^+$ state, the rotational transition intensity was calculated and compared with the observed intensity. We also measured the collision induced rotational relaxation of the N_2^+ ions by changing the delay time between the ionization and probing lasers. Not only the absolute value of the rotational relaxation rate constant, but also the propensity rule due to the symmetry restriction, were obtained. These results show that the resonant enhanced multiphoton ionization combined with the laser induced fluorescence technique is very useful to elucidate the role of the internal states of ions in ion–molecule reactions.

II. EXPERIMENTAL

In this work we used three dye lasers. The first laser light (v_1) pumped N_2 molecule to the $v = 1$ level in the $a\,^1\Pi_g$ state by two-photon absorption. The second laser light (v_2) excited the $a\,^1\Pi_g$ state molecule to the $v = 0$ level of the $c'\,^1\Sigma_u^+$ or the $c\,^1\Pi_u$ state. Then this excited molecule was successively ionized by the absorption of another photon
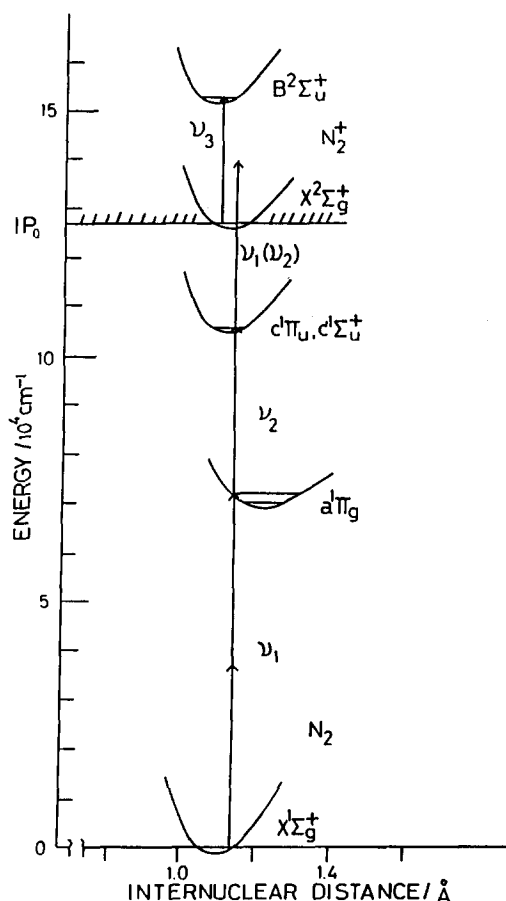
FIG. 1. Potential energy curves of N_2 and N_2^+. Also given are the ionization and the detection scheme. The potential curves were drawn by the reference to the parameters in Ref. 14.

(mainly ν_1). The third laser light (ν_3) was fired at a certain delay time to probe the generated N_2^+ ion by measuring the LIF spectrum of the $B\,^2\Sigma_u^+ \leftarrow X\,^2\Sigma_g^+$ transition.

The experimental arrangement is schematically shown in Fig. 2. A Nd:YAG laser (Quantel YG 581-10) was used to pump two dye lasers (ν_1 and ν_2) simultaneously. The first laser light (ν_1) was the second harmonic of a dye laser (Quantel TDL 50, rhodamine 6G dye) and produced 6 mJ at 283 nm with a linewidth of 0.2 cm^{-1}. The second dye laser light (ν_2) was also a frequency doubled output of another dye laser (Molectron DL 14 with rhodamine B dye) and
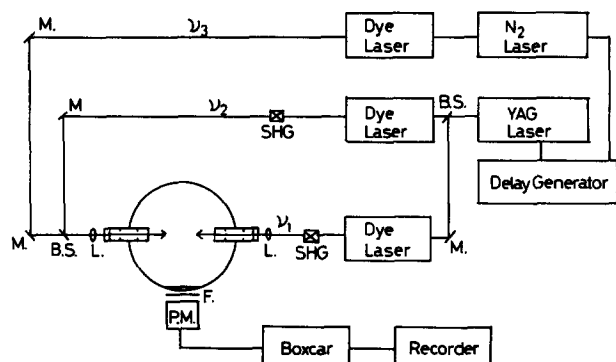

FIG. 2. Experimental setup for the two-color REMPI and laser induced fluorescence detection of the ions.

produced 0.3 mJ at 295 nm with a linewidth of 1 cm^{-1}. The two laser beams were counterpropagated through a gas cell without delay time. The third laser light (ν_3) was a nitrogen laser (Molectron UV 24) pumped dye laser (Molectron DL 14, BBQ dye) with a linewidth of 1 cm^{-1} and typical laser power was ~ 0.5 mJ. The ν_3 beam was introduced coaxially to the first and second laser beams using a beam splitter which reflects UV light and transmits visible light. All the laser beams (ν_1, ν_2, ν_3) are linearly polarized. The direction of the polarization of ν_2 is parallel to ν_3 and perpendicular to ν_1. The delay time between the first and third lasers was changed from 10 to 35 ns (with an uncertainty of ± 2 ns) by the digital delay circuit (BNC model AP-3). The lifetime of the $c'\,^1\Sigma_u^+$ ($v = 0$) state is reported to be 0.9 ns[15] and the $c\,^1\Pi_u$ state is thought to have a same lifetime. Therefore, a probing laser (ν_3) is used only for monitoring the produced ions and does not contribute to the ionization of the c or c' state. The delay time was determined by monitoring the three laser outputs by a fast photodiode (Hamamatsu S1190) combined with a digital oscilloscope (Tektronics 2430). Nitrogen was flowed in the static gas cell at a pressure of 1–3 Torr and the pressure was measured by a capacitance manometer (MKS Baratron). Fluorescence from the $B\,^2\Sigma_u^+$ state of the N_2^+ ion was measured at the right angle to the laser beams by a photomultiplier (Hamamatsu R-928) after passing through filters (Toshiba Y42 and V40). The photocurrent was averaged by a boxcar integrator (Brookdeal 9415/9425 or PAR 4402/4420) and recorded on a chart recorder or the data were processed by a microcomputer and plotted by an x–y plotter.

III. RESULTS AND DISCUSSION

Since the Rydberg states have potential curves almost parallel to that of the ion, the Franck–Condon factor favors the ionization transition of $\Delta v = 0$. The N_2^+ ions photoionized from $c'\,^1\Sigma_u^+$ ($v = 0$) and $c\,^1\Pi_u$ ($v = 0$) are therefore distributed exclusively in the $v = 0$ level of the $X\,^2\Sigma_g^+$ state of the N_2^+ ion, contributing to a large LIF signal of the ions. The selective distribution was also observed by Pratt et al.[16] by their photoelectron study. To determine the nascent rotational distribution of the produced ions in the $v = 0$ level, we have to examine the collisional effect since ions usually have a large quenching cross section.[17–19] Therefore, we first examined the collisional effect by the measurements of the LIF spectra of the N_2^+ ion at different delay times between the ionization laser and the probing laser. Then we determined the relaxation rate constant for N_2 collision and the nascent rotational distribution of the N_2^+ ion produced.

A. Collision induced rotational relaxation

Figure 3 shows the LIF spectra due to the $B\,^2\Sigma_u^+$ ($v' = 0, N'$) $\leftarrow X\,^2\Sigma_g^+$ ($v'' = 0, N''$) transition of the N_2^+ ions measured at different delay times and at different N_2 pressures. The final intermediate state in the ionization process is the same $c'\,^1\Sigma_u^+$ ($v = 0, J = 5$) state for all the spectra. A detailed description of the ionization process is given in Sec. III B. The spectra at the delay times of 10 and 15 ns at 1 Torr of N_2 are almost identical and four rotational peaks of
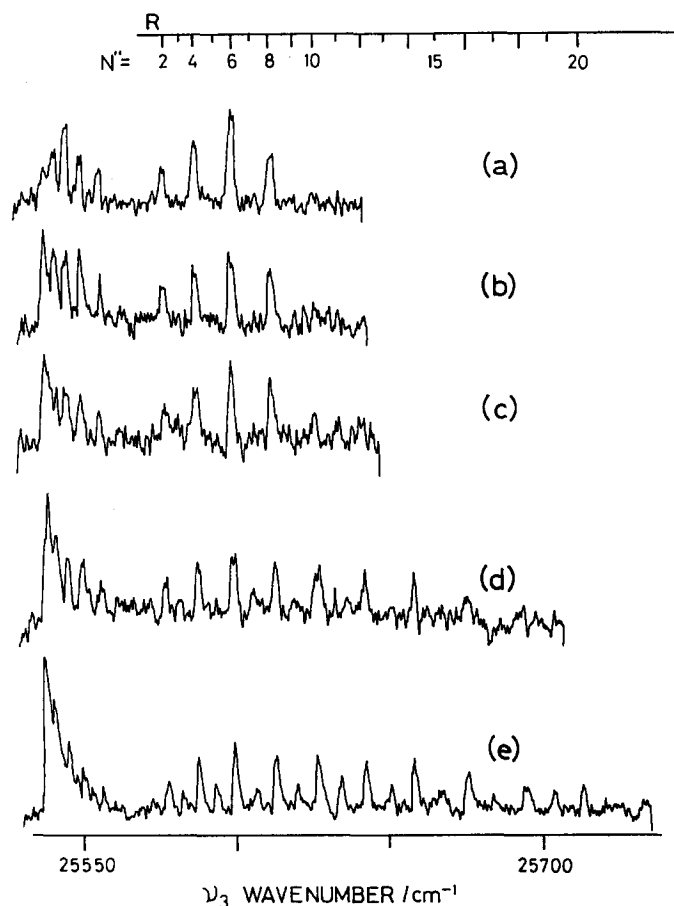
FIG. 3. Laser induced fluorescence spectra of the N_2^+ ions due to the $B\ ^2\Sigma_u^+$ $(v = 0) \leftarrow X\ ^2\Sigma_g^+$ $(v = 0)$ transition measured at several delay times and N_2 pressures. The N_2^+ ions are ionized from the $c'\ ^1\Sigma_u^+$ $[v = 0, J(N) = 5]$ level. The delay time and N_2 pressure are (a) 10 ns and 1 Torr; (b) 15 ns and 1 Torr; (c) 25 ns and 1 Torr; (d) 35 ns and 1 Torr; and (e) 35 ns and 3 Torr.

the R branch corresponding to the transitions from the $N'' = 2, 4, 6$, and 8 rotational levels are identified. As will be discussed later, the initially populated levels are $N'' = 2, 4, 6$, and 8 levels which are the "s" levels with a parity of (+). At the delay time of 25 ns we can clearly see an additional peak due to the transition from $N'' = 10$, and at 35 ns delay time the rotational levels are widely distributed. Within these delay times only even rotational levels are populated and odd rotational levels are hardly seen. Since the even rotational levels have s symmetry, we can conclude that the symmetry and parity restricted selection rule $s(+) \leftrightarrow s(+)$ is obeyed for the collision of the homonuclear diatomic molecule. The same selection rule is reported in other neutral homonuclear molecules such as Na_2 [20] and Li_2.[21] Recently, Sha et al. reported a similar rule for the collisional relaxation of the electronically excited N_2 molecule.[22] This selectivity disappeared at the N_2 pressure of 3 Torr and at the delay time of 35 ns. This is probably due to the occurrence of the multiple collisions.

The rate constant of the rotational relaxation of N_2^+ ions by N_2 collision was calculated by solving the rate equation numerically. Since the spectra obtained at 10 and 15 ns delay times are identical in the spectral intensity distribution, the intensity of the LIF spectrum at the delay time of 10

ns can be assumed to show the initial population of the four levels $N'' = 2, 4, 6$, and 8. The rate constant obtained was 6.4 ($\pm$ 1.5) $\times 10^{-10}$ cm^3 molecule^{-1} s^{-1}. This rate constant is almost equal to the vibrational relaxation,[17] 5×10^{-10} cm^3 molecule^{-1} s^{-1}, showing that the vibrational and the rotational relaxation occur with the same rate.

B. Rotational propensity rule in the ionization and the rotational distribution of the N_2^+ ion

From the previous results it is established that at the delay time less than 15 ns and at the total pressure of 1 Torr, the collisional effect is negligibly small, and we can assume that the LIF spectrum measured at this condition represents the nascent rotational distribution of the N_2^+ ions. For convenience we will label the final intermediate state and the ionic ground state using the subscripts "i" and "f," respectively.

1. Ion [$^2\Sigma_g^+(v=0, J_f, N_f)$] $\leftarrow c'\ ^1\Sigma_u^+(v=0, J_i, N_i)$ transition

Figure 4 shows the LIF spectrum of the N_2^+ ion measured at the delay time of 15 ns and at 1 Torr of N_2. The intermediate rovibronic levels in the ionization process are the same as those chosen in the collisional relaxation measurement described in Sec. III A (Fig. 3). In the spectrum shown in Fig. 4, v_1 is fixed on the $P(6)$ line of the $a\ ^1\Pi_g$ $(v = 1) \leftarrow X\ ^1\Sigma_g^+$ $(v = 0)$ transition and v_2 is fixed on the $Q(5)$ line of the $c'\ ^1\Sigma_u^+$ $(v = 0) \leftarrow a\ ^1\Pi_g$ $(v = 1)$ transition.

The resolution of this spectrum, which is determined by the laser resolution, is ~ 1 cm^{-1}, which is sufficient to clearly resolve the rotational structure of the N_2^+ ion in low N levels. This resolution is far higher than that of the conventional photoelectron spectra. A higher resolution could be achieved easily by use of an étalon. However, in the present spectrum, the separation of the rotational lines is complete and there is no overlap of the lines. Therefore, a quantitative
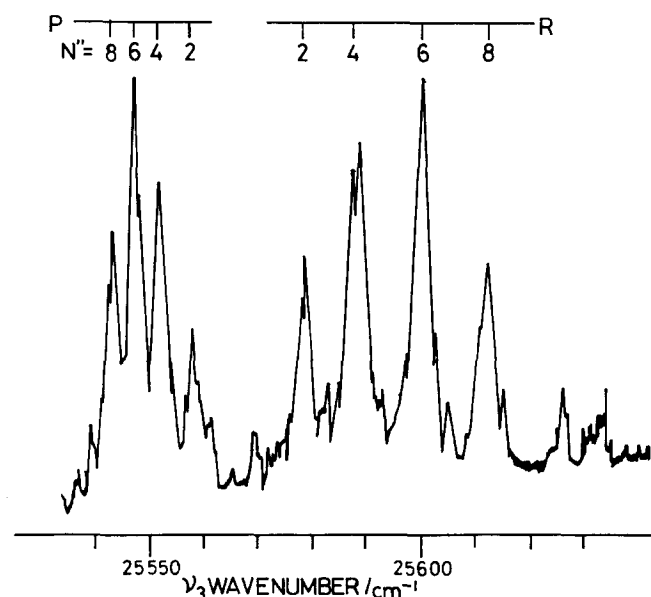

FIG. 4. Laser induced fluorescence spectrum of the N_2^+ $(v = 0)$ ions produced by the ionization from the $c'\ ^1\Sigma_u^+$ $[v = 0, J(N) = 5,$ " $-$ " parity] level. The delay time is 15 ns and the N_2 pressure is 1 Torr.
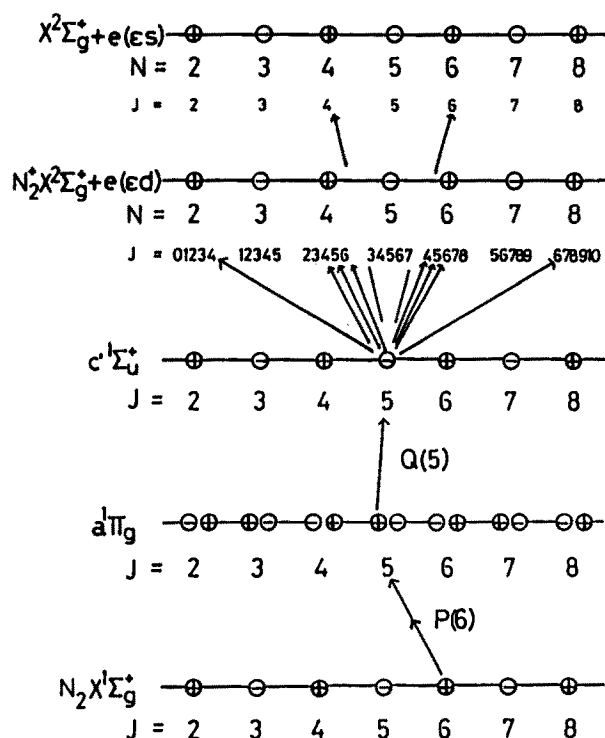
FIG. 5. Allowed rotational transition for the one-photon transition from the $J = N = 5$ ($-$ parity) level of the c' $^1\Sigma_u^+$ state to the X $^2\Sigma_g^+$ state of the ion.

TABLE I. Observed rotational line strength for the transition N_2^+ $(X^2\Sigma_g^+, N_f) + e^- \leftarrow N_2(c\ ^1\Pi_u, N_i)$ and $(c'\ ^1\Sigma_u^+, N_i)$.

State	N_i (parity)	ΔN	Observed intensity[a]
$c'\ ^1\Sigma_u^+$	6(+)	+ 3	0.42
		+ 1	0.73
		− 1	1.00
		− 3	0.73
	5(−)	+ 3	0.37
		+ 1	0.88
		− 1	1.00
		− 3	1.06
$c\ ^1\Pi_u$	2(−)	+ 2	0.26
		0	1.00
		− 2	...
	5(−)	+ 3	0.26
		+ 1	0.82
		− 1	1.00
		− 3	0.79

[a]The intensity is normalized by N_2^+ $(B^2\Sigma_u^+ \leftarrow X^2\Sigma_g^+)$ rotational line strength.

discussion can be made about the rotational branching ratio with the present data.

The N_2^+ ions observed in this spectrum are ionized from the $N_i = 5$ level of the c' $^1\Sigma_u^+$ ($v = 0$) state. The four strong peaks in each of the R and P branches can be easily assigned as the transitions from the $N_f = 2, 4, 6,$ and 8 levels in the $X^2\Sigma_g^+$ ($v = 0$) state of N_2^+ to the allowed rotational levels in the B $^2\Sigma_u^+$ ($v = 0$) state. Therefore, the spectrum clearly shows the existence of a rotational propensity rule $\Delta N = \pm 1, \pm 3$ in the photoionization from the neutral molecule in the c' $^1\Sigma_u^+$ state to the $X^2\Sigma_g^+$ state of the ion. This result agrees with that found by Pratt et al.[7] for the ionization of H_2 from the B $^1\Sigma_u^+$ state and also with that by Viswanathan et al.[10] for the ionizaton of NO from the D $^2\Sigma^+$ state. All the cases represent the ionization from the neutral Σ^+ ($npσ$) Rydberg state to the Σ^+ ionic state. Therefore, the result for N_2 is explained in the same way as that given for

H_2.[7] The observed N_2^+ ions are produced by the photoionization from the c' $^1\Sigma_u^+$ state. Because the c' $^1\Sigma_u^+$ state is the $4pσ$ Rydberg state, the electron ejected by the ionization should have an s or d character because of the $\Delta l = \pm 1$ selection rule. Then the propensity is explained by considering the ionic ground state X $^2\Sigma_g^+$ and the ejected electron by the Hund's coupling case (d). The schematic diagram of the ionization process is shown in Fig. 5. The last step of the ionization process is one-photon absorption. The one-photon dipole transition predicts that the change in total angular momentum of the system (ion + ejected electron) should be $\Delta J = 0, \pm 1$ and the parity should change. This leads to the rotational selection rule $\Delta N = \pm 1, \pm 3$ for the ionization as shown in the figure. The observed rotational intensity distribution is given in Table I. This distribution can be compared with the theoretical calculation.

Several theoretical approaches have been developed for the formulation of the rotational selection rule and the transition intensity of the photoionization of a diatomic molecule.[23-25] The ionization process of the $\Sigma \leftarrow \Sigma$ transition is formulated by Itikawa[23] for the case of the linearly polarized ionization light and can be written as follows:

$$\sigma_{\text{tot}}\,(\gamma_f v_f N_f \leftarrow \gamma_i v_i N_i) = A(2N_f + 1)\Sigma_{\lambda=0,1}\Sigma_{\bar{\lambda}=0,1}(2 - \delta_{\lambda 0})(2 - \delta_{\bar{\lambda}0})(-1)^{\lambda+\bar{\lambda}}$$

$$\times \Sigma_l \left[(2|1-1|+1)\begin{pmatrix} 1 & 1 & |1-1| \\ -\lambda & \lambda & 0 \end{pmatrix}\begin{pmatrix} 1 & 1 & |1-1| \\ -\bar{\lambda} & \bar{\lambda} & 0 \end{pmatrix}\begin{pmatrix} N_f & N_i & |1-1| \\ 0 & 0 & 0 \end{pmatrix}^2 \right.$$

$$\left. + (2l+3)\begin{pmatrix} 1 & 1 & 1+1 \\ -\lambda & \lambda & 0 \end{pmatrix}\begin{pmatrix} 1 & 1 & 1+1 \\ -\bar{\lambda} & \bar{\lambda} & 0 \end{pmatrix}\begin{pmatrix} N_f & N_i & 1+1 \\ 0 & 0 & 0 \end{pmatrix}^2 \right]\langle\langle d^{(\lambda)}\rangle\rangle_1\langle\langle d^{(\bar{\lambda})}\rangle\rangle_1^*,$$

(1)

where $A = 32\pi^4 e^2 v/9c$ and $(::)$ is the 3-j symbol. l is the angular momentum of the ejected electron and λ is its projection to the molecular axis. $\langle\langle d^{(\lambda)}\rangle\rangle_1$ is the integral including vibrational and electronic wave functions,

$$\langle\langle d^{(\lambda)}\rangle\rangle_1 = \langle \chi_{vf}(R)|\chi_{vi}(R)\rangle$$

$$\times \langle \varphi_{\gamma f\Lambda f\lambda}|\Sigma_s r_s Y_{1\mu}(r_s')|\varphi_{\gamma iJi\Lambda iMi}\rangle.$$
(2)

In the present ionization process, we take into account only the electronic part since the Franck–Condon factor favors the $\Delta v = 0$ transition.

Since the c' $^1\Sigma_u^+$ is the $4p\sigma(l = 1)$ Rydberg state, the ejected electron will be an $s(l = 0)$ or $d(l = 2)$ electron. For the ejection of the s electron, we treat only the $l = 0$ (therefore, $\lambda = \bar{\lambda} = 0$) case. Then Eq. (1) becomes very simple and can be reduced as follows:

$$\sigma_{s \text{ electron}} = \mathbf{A}\times 2(2N_f + 1)\begin{pmatrix} N_f & N_i & 1 \\ 0 & 0 & 0 \end{pmatrix}^2$$

$$\times \langle\langle d^{(0)}\rangle\rangle_0\langle\langle d^{(0)}\rangle\rangle_0^*.$$
(3)

By using the symmetry relation of the 3j symbol, the $\Delta N = N_f - N_i = \pm 1$ selection rule is easily derived. For the ejection of the d electron, Eq. (1) becomes

$$\sigma_{d \text{ electron}} = \mathbf{A}(2Nf + 1)\Sigma_{\lambda = 0,1}\Sigma_{\bar{\lambda} = 0,1}(2 - \delta_{\lambda 0})(2 - \delta_{\bar{\lambda}0})(-1)^{\lambda + \bar{\lambda}}$$

$$\times \left[3\begin{pmatrix} 2 & 1 & 1 \\ -\lambda & \lambda & 0 \end{pmatrix}\begin{pmatrix} 2 & 1 & 1 \\ -\bar{\lambda} & \bar{\lambda} & 0 \end{pmatrix}\begin{pmatrix} N_f & N_i & 1 \\ 0 & 0 & 0 \end{pmatrix}^2\right.$$

$$\left. + 7\begin{pmatrix} 2 & 1 & 3 \\ -\lambda & \lambda & 0 \end{pmatrix}\begin{pmatrix} 2 & 1 & 3 \\ -\bar{\lambda} & \bar{\lambda} & 0 \end{pmatrix}\begin{pmatrix} N_f & N_i & 3 \\ 0 & 0 & 0 \end{pmatrix}^2\right]\langle\langle d^{(\lambda)}\rangle\rangle_1\langle\langle d^{(\bar{\lambda})}\rangle\rangle_1^*.$$
(4)

The first term gives the selection of $\Delta N = \pm 1$ and the second term $\Delta N = \pm 1$ and ± 3. Now we have derived the rotational selection rule the same as that obtained by the diagram of Fig. 5. This selection rule was also demonstrated by Dixit and McKoy.[25]

Because we do not have an information of the values of electronic part $\langle\langle d^{(\lambda)}\rangle\rangle_1\langle\langle d^{(\bar{\lambda})}\rangle\rangle_1^*$, only the rotational part has been calculated and the results for the transition from c' $^1\Sigma_u^+$, $v_i = 0$, $N_i = 5$ are listed in Table II. To discuss it more completely, we have to take into account the alignment of the molecule produced by the linearly polarized lasers in addition to the integrals of the electronic part. Nevertheless, apart from the change of sign, the results give us reasonable estimation of the rotational transition intensity. From Table II we can expect that the $\Delta N = +1$ transition is almost equal in intensity to the $\Delta N = -1$ transition and relatively stronger than those of the $\Delta N = \pm 3$ transitions, showing a good agreement with the observed result given in Table I.

2. Ion [²Σ⁺_g (v=0,Jₜ,Nₜ)]←c ¹Πᵤ (v=0,Jᵢ,Nᵢ) transition

Figure 6 shows the LIF spectrum due to the same electronic transition of N_2^+. In this case, ν_1 is fixed on the $P(2)$ line of the a $^1\Pi_g$ $(v = 1) \leftarrow X$ $^1\Sigma_g^+$ $(v = 0)$ transition and ν_2 is fixed on the $R(1)$ line of the c $^1\Pi_u$ $(v = 0)\leftarrow a$ $^1\Pi_g$ $(v = 1)$ transition. Therefore, the N_2^+ ions are produced by the ionization from the $N = 2$ [$(-)$ parity] level of the c $^1\Pi_u$ $(v = 0)$ state. The observed peaks in the spectrum are

assigned to the P and R branches due to the transitions from the $N = 2$ and 4 levels of X $^2\Sigma_g^+$ of N_2^+. This suggests the rotational propensity rule of $\Delta N = 0, \pm 2$ for the ionization. The intensity of the rotational peak $R(0)$, which corresponds to the production of the $N = 0$ level by $\Delta N = -2$, is
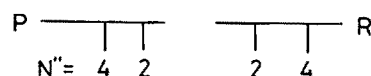

TABLE II. Calculated rotational intensity for the transition N_2^+ $(^2\Sigma_g^+,N_f) + e^- \leftarrow N_2(^1\Sigma_u^+, N_i = 6)$. To obtain the absorption cross section, these values should be multiplied by $32\pi^4 e^2 v/9c$ and the electronic term, $\langle\langle d^{(\lambda)}\rangle\rangle_1\langle\langle d^{(\bar{\lambda})}\rangle\rangle_1^*$ (see the text).

l	λ	$\bar{\lambda}$	ΔN			
			-3	-1	$+1$	$+3$
0ᵃ	0	0		0.92	1.1	
2ᵇ	0	0	0.14	0.29	0.35	0.23
	0	1	-0.16	0.19	0.23	-0.27
	1	0	-0.16	0.19	0.23	-0.27
	1	1	0.19	0.69	0.81	0.30

ᵃ This case corresponds to the ejection of the s electron.
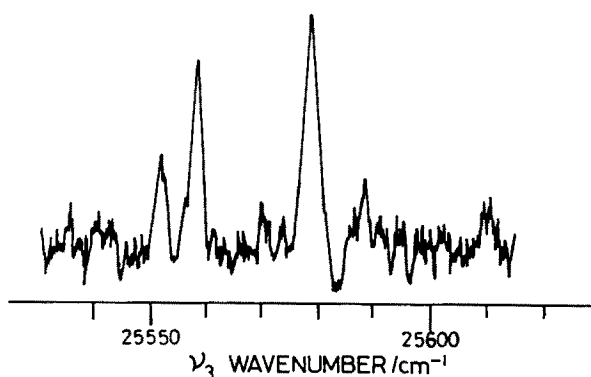ᵇ This case corresponds to the ejection of the d electron.

FIG. 6. Laser induced fluorescence spectrum of the N_2^+ $(v = 0)$ ions produced by the ionization from the c $^1\Pi_u$ $[v = 0, J(N) = 2, -$ parity] level. The delay time is 15 ns and the N_2 pressure is 1 Torr.

very weak. This is due to a small Hönl–London factor for $R(0)$ compared with the other peaks in the spectrum. [The values of Hönl–London factors for $R(0)$, $R(2)$, and $R(4)$ are 1, 3, and 5, respectively.]

The c $^1\Pi_u$ state is the $3p\pi$ Rydberg state. The photoionization from this state is depicted in Fig. 7. From this scheme the rotational propensity rule $\Delta N = 0$, ± 2 is derived by a way similar to the case of ionization from the c' $^1\Sigma_u^+$ state. The rotational level chosen in the c $^1\Pi_u$ state in Fig. 6 corresponds to the Π^- component as is seen in Fig. 7. We can derive another propensity in the transition from the Π^+ component by suitable selection of the rotational lines by the ν_1 and ν_2 laser light. The propensity is clearly demonstrated in Fig. 8, where N$_2$ is ionized from the $J(N) = 5$ [($-$) parity] level belonging to the Π^+ component of the c $^1\Pi_u$ state. The ionization from the Π^+ component produces four rotational levels of the ion by the $\Delta N = \pm 1$, ± 3 propensity rule. Such a difference in the rotational propensity in photoionization from the different component of the Π state was also found in the ionizations from the C $^2\Pi$ state of NO by Viswanathan et al.[10] and from the c $^1\Pi_u$ state of H$_2$ by O'Halloran et al.[8]

3. Effect of the perturbation

The rotational propensity in photoionization reflects the electronic character of the final intermediate state of ionization process. The c' $^1\Sigma_u^+$ and c $^1\Pi_u$ states, which are selected as the final intermediate states in the experiment, are not the pure Rydberg states. In the energy region near the c' $^1\Sigma_u^+$ ($4p\sigma$ Rydberg) and c $^1\Pi_u$ ($3p\pi$ Rydberg) states, there is another Rydberg state [o $^1\Pi_u$ ($3s\sigma$ Rydberg)] and two valence states (b' $^1\Sigma_u^+$ and b $^1\Pi_u$). These five highly
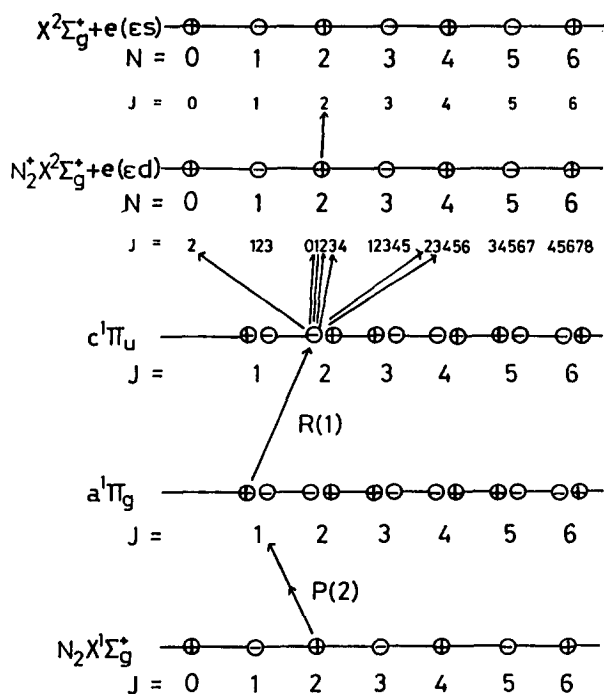

FIG. 7. Allowed rotational transition for the one-photon transition from the $J = N = 2$ ($-$ parity) level of the c $^1\Pi_u$ state to the X $^2\Sigma_g^+$ state of the ion. This level belongs to the Π^- component.
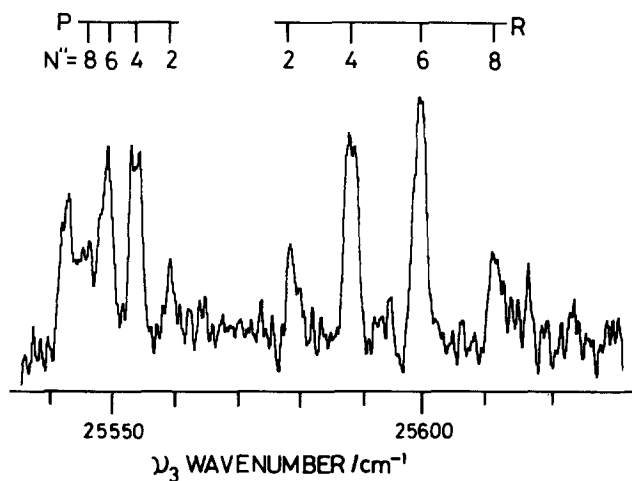

FIG. 8. Laser induced fluorescence spectrum of the N$_2^+$ ($v = 0$) ions produced by the ionizaton from the c $^1\Pi_u$ [$v = 0$, $J(N) = 5$, $-$ parity] level. This level belongs to the Π^+ component. The delay time is 15 ns and the N$_2$ pressure is 1 Torr.

excited states of N$_2$ molecule mix with each other by heterogeneous and homogeneous perturbations.[26–30] The effect of the mixing on the rotational propensity will be considered.

For the c' $^1\Sigma_u^+$ ($v = 0$) state, Stahel et al. reported that this $3p\sigma$ Rydberg state contains 1.7% of the b $^1\Sigma_u^+$ (valence) character.[30] The ratio of the mixing is too small to find any peaks indicating the valence character in the present spectrum. They also showed that the c $^1\Pi_u$ ($v = 0$) state contains 63.9% of the b $^1\Pi_u$ (valence) and 1.9% of the o $^1\Pi_u$ ($3s\sigma$ Rydberg) characters. However, the production of N$_2^+$ in the X $^2\Sigma_g^+$ electronic state from the b $^1\Pi_u$ and o $^1\Pi_u$ states requires the excitation of two electrons by considering the electronic configuration of the states.[31,32] Therefore, only the c $^1\Pi_u$ state character dominates in the transition from this mixed state, causing no violation of the propensity.

As was demonstrated in our previous paper[13] and also shown by other workers,[26–29] there exists a strong heterogeneous perturbation between the c' $^1\Sigma_u^+$ and c $^1\Pi_u$ states, i.e., Λ-type doubling. The c' $^1\Sigma_u^+$ state interacts with the Π^+ component of the c $^1\Pi_u$ state and not with the remaining Π^- component. As is seen in the ionization schemes of Figs. 5 and 7, the ionizations from the $^1\Sigma_u^+$ and $^1\Pi^+$ states give the same rotational propensity $\Delta N = \pm 1$, ± 3. Therefore, the heterogeneous perturbation between the c' $^1\Sigma_u^+$ and c $^1\Pi_u$ states does not affect the rotational propensity. However, the perturbation can affect the intensity distribution for the transition. As can be seen in Table I, almost the same intensity distribution was obtained from the ionizations of the $N = 5$ level of the c' $^1\Sigma_u^+$ and of the $N = 5$ level of the c $^1\Pi_u$ state. Since the two levels are mixed with each other, it is reasonable that the two spectra show identical results.

In conclusion we have measured the LIF spectra of the N$_2^+$ ions produced by double resonant MPI and found the rotational properties in the photoionization from the c' $^1\Sigma_u^+$ and c $^1\Pi_u$ states of the neutral molecule. These propensities and rotational intensity distribution agree with the theoretical predictions. No effect of the state mixing in the final

intermediate state in the photoionization is observed. The collision induced rotational relaxation rate constant of the N_2^+ ions by N_2 was determined and the symmetry selection rule $s(+)\leftrightarrow s(+)$ [" $a(-)$ " $\leftrightarrow$ " $a(-)$ "] was found to be obeyed. Finally we would like to emphasize that the combination of the laser induced fluorescence and resonance enhanced multiphoton ionization provides us with a powerful tool for the determination of the internal state of ions. We are planning to study the internal state dependence on ion–molecule reactions by using this technique.

[1] Y. Achiba, K. Sato, K. Shobatake, and K. Kimura, J. Chem. Phys. 78, 5474 (1983).

[2] W. E. Conaway, R. J. S.Morrison, and R. N. Zare, Chem. Phys. Lett. 113, 429 (1985).

[3] S. T. Pratt, P. M. Dehmer, and J. L. Dehmer, J. Chem. Phys. 80, 1706 (1984).

[4] L. Åsbrink, Chem. Phys. Lett. 7, 549 (1970).

[5] Y. Morioka, S. Hara, and M. Nakamura, Phys. Rev. A 22, 177 (1980).

[6] J. E. Pollard, D. J. Trevor, J. E. Reutt, Y. T. Lee, and D. A. Shirley, J. Chem. Phys. 77, 34 (1982).

[7] S. T. Pratt, P. M. Dehmer, and J. L. Dehmer, J. Chem. Phys. 78, 4315 (1983).

[8] M. A. O'Halloran, S. T. Pratt, P. M. Dehmer, and J. L. Dehmer, J. Chem. Phys. 87, 3288 (1987).

[9] W. G. Wilson, K. S. Viswanathan, E. Sekreta, E. R. Davisón, and J. P. Reilly, J. Phys. Chem. 88, 672 (1984).

[10] K. S. Viswanathan, E. Sekreta, E. R. Davison, and J. P. Reilley, J. Phys. Chem. 90, 5078 (1986).

[11] K. Müler-Dethlefth, M. Sander, and E. W. Schlag, Chem. Phys. Lett. 112, 291 (1984).

[12] For example, Reilly's group get the resolution of 3 meV by using time-of-flight apparatus (see Ref. 10).

[13] T. Ebata, A. Fujii, and M. Ito, J. Phys. Chem. 91, 3125 (1987).

[14] K. P. Huber and G. Herzberg, Molecular Spectra and Molecular Structure, Vol. IV (Van Nostrand Reinhold, New York, 1979).

[15] J. E. Hesser and K. Dressler, J. Chem. Phys. 45, 3149 (1966).

[16] S. T. Pratt, P. M. Dehmer, and J. L. Dehmer, J. Chem. Phys. 81, 3444 (1984).

[17] E. E. Ferguson, J. Phys. Chem. 90, 731 (1986).

[18] W. Federer, W. Dobler, F. Howorka, W. Lindinger, M. Durup-Ferguson, and E. E. Ferguson, J. Chem. Phys. 83, 1032 (1985).

[19] H. Böhringer, M. Durup-Ferguson, D. W. Fahey, F. C. Fehsenfeld, and E. E. Ferguson, J. Chem. Phys. 79, 4201 (1983).

[20] K. Bergmann and W. Demtröder, Zh. Phys. 243, 1 (1971).

[21] Ch. Ottinger, R. Velasco, and R. N. Zare, J. Chem. Phys. 52, 1636 (1970).

[22] G. Sha, D. Proch, and K. Kompa, J. Chem. Phys. 87, 5251 (1987).

[23] Y. Itikawa, Chem. Phys. 28, 461 (1978).

[24] S. N. Dixit and V. McKoy, J. Chem. Phys. 82, 3546 (1985).

[25] S. N. Dixit and V. McKoy, Chem. Phys. Lett. 128, 49 (1986).

[26] P. K. Carrol and C. P. Collins, Can. J. Phys. 47, 563 (1969).

[27] K. Dressler, Can. J. Phys. 47, 547 (1969).

[28] H. Lefebre-Brion, Can. J. Phys. 47, 541 (1969).

[29] N. W. Leoni, Dissertation No. 4939 ETH, Zurich, 1972.

[30] D. Stahel, M. Leoni, and K. Dressler, J. Chem. Phys. 79, 2541 (1983).

[31] A. Lofthus and P. H. Krupenie, J. Phys. Chem. Ref. Data 6, 113 (1977).

[32] H. H. Michels, Adv. Chem. Phys. 45, 225 (1981).